Design and Calibration of a CW Time Reversal Wireless Power Transfer Transmitter with Pilot Signal Detection

Young-Seok Lee[#1], Taeyeong Yoon[#2], Jungsuek Oh[#3], and Sangwook Nam[#4]

[#]Wave Fusion Lab., Dept. of Electrical and Computer Eng., Seoul National University, Republic of Korea

{[1]ryanlee, [2]taeyeong.yoon, [3]jungsuek, [4]snam}@snu.ac.kr

2025 Asia-Pacific Microwave Conference (APMC) | 979-8-3315-3455-4/25/$31.00 ©2025 IEEE | DOI: 10.1109/APMC65046.2025.11378159

***Abstract*— This paper presents a Continuous Wave (CW) Wireless Power Transfer (WPT) transmitter system capable of detecting pilot signals via a novel hardware calibration method and validated by Time Reversal (TR) algorithm. The proposed transmitter architecture integrates a frequency-offset-based pilot signal detection scheme and compensates for all path-dependent distortions through a one-time calibration process. A Look-Up Table (LUT) is generated using simulation-derived ideal values, enabling accurate estimation of the pilot signal's magnitude and phase at the transmitter array (TXA). The system is implemented with a 16×16 TXA and a 5×5 receiver array (RXA), operating at 5.64 GHz with a 7 kHz pilot offset. The calibration and TR focusing performance are validated through experiments comparing measured and simulated results. This foundational study provides a scalable and practical method for efficient WPT calibration technique in pilot signal-based TR systems.**

***Keywords*— Array Calibration, Fast Fourier Transform (FFT), Retrodirective, Time Reversal (TR), Wireless Power Transfer (WPT).**

I. Introduction

Wireless Power Transfer (WPT) technology has become increasingly promising due to advances in electronic devices and their widespread adoption [1], [2]. Especially, radiative WPT systems can deliver electromagnetic beams to receivers over various distances, from short to long range. A major objective of WPT technology is to efficiently direct power beams toward the intended receiver. One effective approach is to detect pilot signals transmitted from the receiver elements, which provides magnitude and phase information. Fig. 1 well illustrates the conventional process.

Time Reversal (TR) and retrodirective topology are the most well-known signal processing methods for this purpose [3], [4], [5]. While TR processes signals by flipping the received time-domain response and is more suitable for pulsed and multi-path environments, retrodirective simply conjugates the received signal and are better suited for Continuous Wave (CW) scenarios. However, in free-space environments with no obstacles and CW operation, both methods yield equivalent results. This paper expresses as the TR terminology as it represents a more general framework while maintaining the same functionality in CW scenarios.

This paper presents a hardware architecture and calibration method for detecting pilot signals in TR-based WPT systems. The proposed approach is validated through experimental measurements of TR pattern power delivery to the receiver,

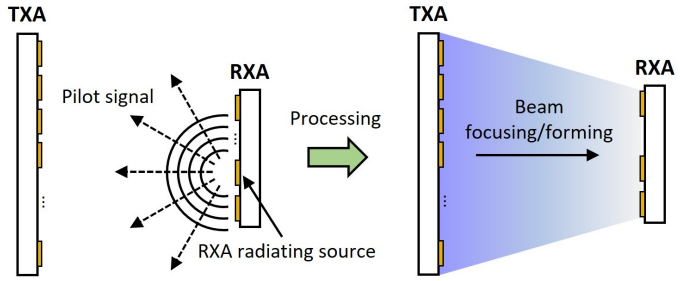

Fig. 1. Illustration of conventional pilot signal detection and following power beamfocusing/forming process.

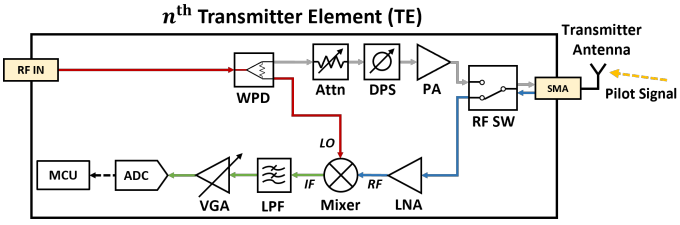

Fig. 2. Block diagram of the Transmitter Element (TE).

with results compared against simulations. Section II describes the system structure and calibration topology, Section III presents the measured results with simulation comparisons, and Section IV concludes the paper.

II. Calibration Topology

A. Scenario

Fig. 2 shows the block diagram of a Transmitter Element (TE). The Transmitter Array (TXA) consists of multiple TEs, corresponding to the number of array elements. Each TE is fed with an RF input signal through distribution networks from an RF source. The gray path indicates the conventional power transmission path, where the signal's magnitude and phase are controlled, then amplified and transmitted. In contrast, the red (LO), blue (RF), and green (IF) paths represent the path that are engaging pilot signal detection.

B. Calibration Methodology

The main objective of the proposed calibration topology is to eliminate all the phase delays and magnitude attenuation / amplification in the path and to detect an accurate pilot signal,

since the signal distribution to each TE is different, as is the circuit of each TE itself. That is, to obtain the aggregated magnitude and phase information along the red, blue, and green paths and save it as a Look-up Table (LUT). Then, when the pilot signal is detected at the MCU, it can be compensated by subtracting the effects of the paths using LUT, thereby obtaining the accurate magnitude and phase information of the pilot signal at the transmitter antenna.

The basic pilot signal detection topology is based on a conventional method, where the key idea is to use a frequency offset in the pilot signal. Let the system operating frequency be ω_0, which is the center frequency. The signal from 'RF IN', corresponding to the red path, operates at frequency ω_0. The pilot signal, however, operates at $\omega_0 + \Delta\omega$, where $\Delta\omega$ is a frequency offset much smaller than ω_0 ($\Delta\omega \ll \omega_0$), such that it is ignorable enough to affect the center frequency operation.

Assume the pilot signal is radiated as $Ae^{j(\omega_0+\Delta\omega)t}$ at the receiver antenna. Due to propagation, phase delay and magnitude attenuation occur, so the transmitter antenna at the n^{th} TE receives $A_n e^{j(\omega_0+\Delta\omega)(t-\tau_n)}$. Recall that the goal of the calibration is to accurately detect A_n and $\psi_n = -(\omega_0+\Delta\omega)\tau_n$. Passing through the blue path, the RF signal at the mixer, denoted as S_{RF}, can be written as follows:

$$S_{RF} = A_n a_n e^{j[(\omega_0+\Delta\omega)(t-\tau_n)-\alpha_n]} \tag{1}$$

where a_n and α_n are the magnitude and phase changes during the path, respectively. Using the same notation, the LO signal before the mixer, denoted as S_{LO}, can be written as follows:

$$S_{LO} = B_n e^{j(\omega_0 t-\beta_n)} \tag{2}$$

where B_n and β_n are the magnitude and phase changes during the path all the way from the RF source, respectively. Then, the mixed and down-converted signal at frequency $\Delta\omega$, after the VGA, denoted as S_{ADC}, can be expressed as follows:

$$S_{ADC} = \frac{A_n a_n B_n C_n}{2} \cdot e^{j\Delta\omega t} e^{-j((\omega_0+\Delta\omega)\tau_n+\alpha_n+\beta_n+\gamma_n)} \tag{3}$$

where C_n and γ_n are the magnitude and phase changes during the green path, respectively. As this signal passes through the Analog-to-Digital Converter (ADC), it is quantized and subsequently processed. By using the Fast Fourier Transform (FFT), the magnitude and phase of equation (3) can be derived. Therefore, after computing the FFT, the following results are obtained:

$$M_n = (A_n a_n B_n C_n)/2 \tag{4}$$

$$\varphi_n = -((\omega_0 + \Delta\omega)\tau_n + \alpha_n + \beta_n + \gamma_n) \tag{5}$$

The LUT can be generated and saved as shown in Table 1. The basic idea is to eliminate A_n and ψ_n through theoretical (ideal) calculations from equations (4) and (5), and store the results in the LUT. The ideal pilot signal can be calculated using the Friis equation and the measured antenna radiation pattern [6]. When another pilot signal is received at an arbitrary location, it can be detected by compensating the measured results using the following equations.

$$A_n^* = M_n^*/\lambda_n \tag{6}$$

Table 1. LUT calculation and its saved information (λ_i and θ_i) for each TEs.

magnitude info. (λ_i)	**phase info.** (θ_i)
$\lambda_1 = M_1/A_1$	$\theta_1 = \varphi_1 - (-(\omega_0 + \Delta\omega)\tau_1)$
$\lambda_2 = M_2/A_2$	$\theta_2 = \varphi_2 - (-(\omega_0 + \Delta\omega)\tau_2)$
$\vdots$	$\vdots$
$\lambda_n = M_n/A_n$	$\theta_n = \varphi_n - (-(\omega_0 + \Delta\omega)\tau_n)$

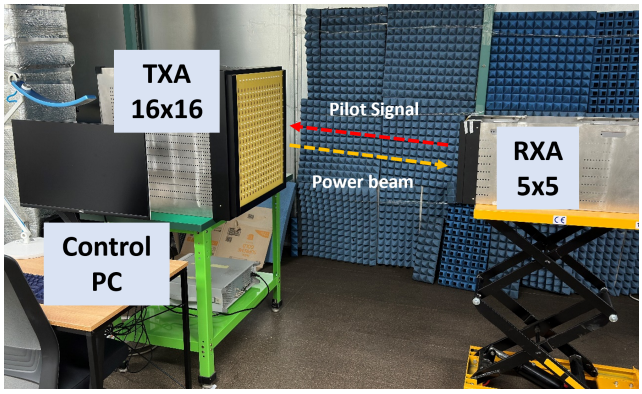

Fig. 3. Hardware setup for TR-WPT experiment.

$$\psi_n^* = \varphi_n^* - \theta_n \tag{7}$$

where the asterisk (*) denotes the pilot signal at an arbitrary location.

III. Results

The experiment was conducted by receiving a pilot signal at the RXA and resending a TR pattern back to the RXA, specifically by simply scaling the magnitude and conjugating the phase. The experimental procedure is summarized as follows:

1) The pilot signal is sent to the TXA from the single antenna of the RXA.
2) The TXA receives the pilot signal and performs calibration using LUT to obtain the magnitude and phase distribution.
3) The magnitude is scaled by normalizing to 20 dBm, and the phases are conjugated to form a TR pattern.
4) Power is transmitted to the RXA and measured using a spectrum analyzer.

Fig. 3 shows the hardware setup. The detailed hardware configuration and operation are well described in [7], [8]. The system operates at 5.64 GHz (ω_0), with a 16×16 TXA and a 5×5 RXA. The magnitude can be attenuated by up to 31.75 dB, and the phase resolution is 22.5°. The frequency offset of the pilot signal ($\Delta\omega$) was set to 7 kHz, which is small enough compared to the center frequency. The ADC operates with 10-bit resolution, capturing 100 quantized samples for FFT calculation.

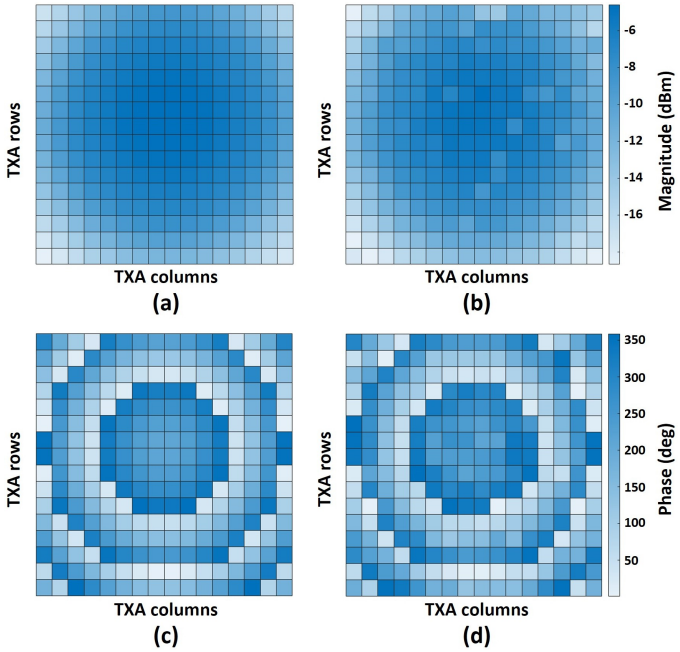

Fig. 4. Received magnitude and phase distribution of the pilot signal at the TXA. (a) and (c) show the ideal magnitude and phase obtained by simulation, while (b) and (d) show the measured magnitude and phase.

Fig. 4 shows the received pilot signal at approximately 0.6 m distance between the TXA and RXA[1]. The pilot signal was radiated at 20 dBm by a signal generator through the single antenna of the RXA. Figures (a) and (c) show the heatmaps of the simulated magnitude and phase distributions, respectively, while (b) and (d) show the corresponding measured and calibrated results. The results exhibit strong similarity, considering the radiation pattern of a single patch antenna and its radiated power.

Fig. 5 shows the received power pattern at the RXA. During the power transmission process, the magnitude was normalized to 20 dBm and the phase was conjugated. Figure (a) shows the simulated result, which was obtained using the ideal patterns from Fig. 4(a) and (c). It exhibits a well-defined focal point at the radiation target, indicating that the TR process was effective. The measured result in (b) also shows a clear focal point, although it is slightly less sharp due to calibration errors or environmental factors during measurement.

IV. Conclusion and Future Works

The most critical challenge in WPT is to determine the location of the RXA or to generate a beam pattern that focuses toward it. Among various approaches, using a pilot signal is one of the simplest and most widely adopted methods. This paper proposed a conventional hardware architecture capable of detecting pilot signal information at the TXA, incorporating

[1]The TXA and RXA are intentionally misaligned to generalize the experimental scenario. The ideal pattern was generated by measuring the exact positions after the experiment. As shown in Fig. 4, the center of the measured distribution is slightly shifted upward from the geometric center.

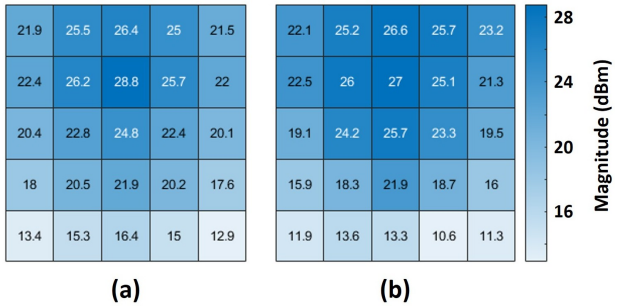

Fig. 5. Received power distribution in dBm. (a) Ideal results by simulation and (b) measured result.

a novel calibration method. The proposed calibration involves all path characteristics—including those from RF signal distribution, paths, and circuit—within a single calibration procedure. Its validity was confirmed through comparison with ideal patterns and experimentally verified by transmitting a basic magnitude scaling-based TR pattern to the RXA.

Although the experimented simple TR pattern does not yield high RF-to-RF efficiency, it provides a foundational result. For practical deployment, further fast post-processing technique development is necessary. By applying additional processing, it is expected that more efficient and real-time energy delivery to the RXA can be achieved [9].

Acknowledgment

This work was supported by Institute of Information & Communications Technology Planning & Evaluation (IITP) grant funded by the Korea government (MSIT) (No. 2019-0-00098, Advanced and integrated software development for electromagnetic analysis).

References

[1] Q. Wu, X. Guan, and R. Zhang, "Intelligent reflecting surface-aided wireless energy and information transmission: An overview," *Proc. IEEE*, vol. 110, no. 1, pp. 150–170, 2022.

[2] B. Strassner and K. Chang, "Microwave power transmission: Historical milestones and system components," *Proc. IEEE*, vol. 101, no. 6, pp. 1379–1396, 2013.

[3] Y.-S. Lee, J. Oh, and S. Nam, "An effect of time reversal based multiple beacon selection on wireless power transfer performance," in *Proc. 2024 Int. Symp. Antennas and Propag. (ISAP 2024)*, Incheon, Republic of Korea, 2024, pp. 1–2.

[4] L. Hu *et al.*, "Auto-tracking time reversal wireless power transfer system with a low-profile planar RF-channel cascaded transmitter," *IEEE Trans. Ind. Electron.*, vol. 70, no. 4, pp. 4245–4255, 2023.

[5] H. Koo *et al.*, "Retroreflective transceiver array using a novel calibration method based on optimum phase searching," *IEEE Trans. Ind. Electron.*, vol. 68, no. 3, pp. 2510–2520, 2021.

[6] H. Y. Kim, Y.-S. Lee, and S. Nam, "Efficiency bound estimation for a practical microwave and mmwave wireless power transfer system design," *J. Electromagn. Eng. Sci.*, vol. 23, no. 1, pp. 69–74, 2023.

[7] Y.-S. Lee *et al.*, "A design and characterization method of a scalable large transmitting array for wireless power transfer," *IEEE Trans. Microw. Theory Techn.*, vol. 73, no. 6, pp. 3346–3358, 2025.

[8] Y.-S. Lee *et al.*, "LUT-based transmit mode calibration complexity reduction method for wireless power transfer," in *Proc. 2024 IEEE Wireless Power Technol. Conf. Expo (WPTCE 2024)*, Kyoto, Japan, 2024, pp. 137–141.

[9] Y.-S. Lee, T. Yoon, Y. J. Song, S. K. Hong, J. Oh, and S. Nam, "Transmission-conversion efficiency maximization technique for MIMO wireless power transfer systems in ISAC applications," *IEEE Antennas Wireless Propag. Lett.*, early access, Jun. 9, 2025.